THE VARIABLE DEPTH-TO-DIAMETER RATIOS OF CANDIDATE IMPACT CRATERS ON BENNU: INFERENCES AND IMPLICATIONS. R.T. Daly[1], E.B. Bierhaus[2], O.S. Barnouin[1], M.E. Perry[1], C.M. Ernst[1], E.E. Palmer[3], R.W. Gaskell[3], J.R. Weirich[3], H.C.M. Susorney[4], C.L. Johnson[3,4], M.G. Daly[5], K.J. Walsh[6], M.C. Nolan[7] and D.S. Lauretta[7]. [1]Johns Hopkins Univ. Applied Physics Laboratory, Laurel, MD, USA (terik.daly@jhuapl.edu); [2]Lockheed Martin Space, Littleton, CO, USA; [3]Planetary Science Institute, Tucson, AZ, USA; [4]Dept. of Earth, Ocean & Atmospheric Sciences, Univ. of British Columbia, Vancouver, Canada; [5]The Centre for Research in Earth and Space Science, York Univ., Toronto, Ontario, Canada; [6]Southwest Research Institute, Boulder, CO, USA; [7]Lunar Planetary Laboratory, Univ. of Arizona, Tucson, AZ, USA.

Introduction: OSIRIS-REx revealed that the asteroid Bennu has hundreds of candidate impact craters [1], henceforth called "impact craters" for simplicity. Impact craters provide clues to the physical properties of Bennu's surface, the age of the surface, and the processes that have shaped Bennu into its present state. They also yield insights into cratering mechanics. Cratering on Bennu occurs in a challenging regime: gravity is very weak [2, 3]; target strength is quite low [2,3], but poorly known, and could vary with depth; target porosity is high [3,4]; and the target surface is very coarse-grained and boulder-rich [2,5]. Here we assess impact crater depth-to-diameter ratios, *d/D*, to characterize impact craters on Bennu and better understand impact processes on rubble-pile asteroids.

Methods: The OSIRIS-REx mission produces shape models and DTMs using two primary techniques: stereophotoclinometry (SPC) and the OSIRIS-REx Laser Altimeter (OLA) [4]. We produced regional DTMs of each impact crater using both methods. Two DTMs per crater were derived from SPC (the first based on a model from January 2019 called v20 and the second based on a mature, higher-resolution model from July 2019 called v34); a third DTM was made from individual OLA scans. The SPC DTMs have a ground-sample distance (GSD) of 44 cm (Jan. 2019) and 15 cm (June 2019), respectively. The OLA DTMs have a 10 cm GSD. We focus on craters >10 m in diameter to ensure that the craters are adequately represented in the v20 DTMs. 84 impact craters exceeded this size threshold; 71 were suitable for *d/D* analysis. Craters were excluded for reasons such as overlap with another depression.

From each regional DTM, we extracted topographic profiles across each crater at eight different azimuths. Rim-to-rim diameter and rim-to-floor depth were determined along each profile. At times, individual profiles were excluded because they passed through an irregularity (e.g. large boulder) on the rim. The remaining profiles were averaged to compute the rim-to-rim diameter, rim-to-floor depth, and *d/D* for each crater.

The irregular shapes and morphologies of impact craters on Bennu pose challenges to analysis. As a second assessment of crater diameter and depth, we mapped the crater rim in each DTM and determined the best-fit ellipse to the rim. The equivalent diameter of this ellipse provided a second estimate of rim-to-rim diameter. The difference between best-fit plane fit to the mapped crater rim and maximum depth within the ellipse provided a second estimate for rim-to-floor crater depth. The profile- and plane-based methods yield consistent results in most cases. However, given Bennu's rubble-rich surface, the best-fit plane method more accurately captures the measurement uncertainties.

Results: Impact craters on Bennu have a range of *d/D* values (Fig. 1). With respect to elevation, *d/D* varies from 0.06 to 0.27. Craters of a given size can exhibit a range of depths. *d/D* is not strongly correlated with the latitude or longitude of the crater. The range of *d/D* in craters depends on crater size (Fig. 2).

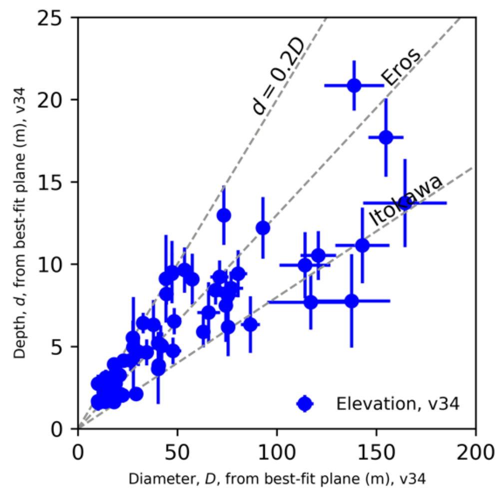

Figure 1. The diameters and depths of craters larger than 10 m on Bennu. As points of reference, dashed lines indicate the *d/D* ratios for typical terrestrial planets (d=0.2D), the asteroid Eros, and rubble pile Itokawa.

The v20 and v34 crater DTMs yield similar trends. The additional detail afforded by the v34 topography improved the measurements of the craters smaller than ~20 m in diameter. OLA comparisons are ongoing; for the craters that have had OLA DTMs generated to date, the results from all three DTMs are consistent (Fig. 3).

Discussion: Many craters on Bennu are shallower than the *d/D* ~0.2 typical of fresh, simple craters on the terrestrial planets. These lower *d/D* ratios are more consistent with results from Itokawa [6] and Eros [7]. The *d/D* ratios of fresh, bowl-shaped impact craters on Ryugu range from 0.14 to 0.2 [8]. While many Bennu craters have *d/D* within this range (Fig. 2), others, including the largest craters, fall outside this range.

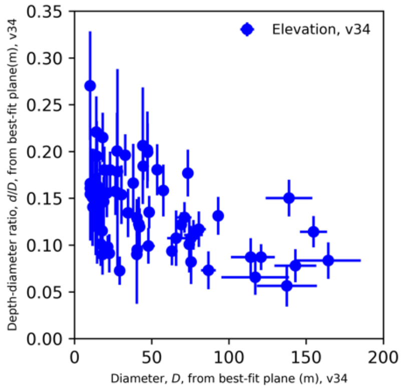

Figure 2. The *d/D* of impact craters as a function of crater size. The range of *d/D* values narrows as crater size increases from 10 to ~100 m. The smallest craters (less than ~30 m) are some of the deepest; the shallowest craters are also among the largest.

Two fundamental questions emerge from the *d/D* data. First, why do craters of a given size show such diverse *d/D* ratios? Second, why does *d/D* appear to vary with crater size?

The range of *d/D* ratios for a given crater size could reflect several factors. Variations in degradation are one possibility. Post-impact modification (e.g., infill) could reduce *d/D*; such a process would not explain why some craters are so deep. Future work will include a detailed analysis of *d/D* on Bennu as a function of crater freshness attributes. That analysis will refine comparisons between the crater populations on Bennu and Ryugu. On Bennu, the steepest slopes are currently located at the midlatitudes [3], but no strong correlation is observed between latitude and *d/D*. A range of *d/D* may be a natural outcome of impacts into coarse-grained targets, even if cratering efficiency is unaffected [9]. In this regime, changes in the geometry of the first contact between target and projectile, as well as the connectivity of target grains, can create a broad range of outcomes from similar initial impact conditions [10]. Variations in target properties such as porosity and strength affect impactor penetration and coupling [11] and could also lead to a range of *d/D*.

The change in *d/D* as a function of crater size (Fig. 2) could reflect several factors. If the small, deep craters are the anomalous ones, then some of the factors described above may be at work. However, if the large, shallow craters are the anomalous ones, then the strength of Bennu may increase with depth. An interplay between strength and gravity as a function of crater size [e.g., 12] could also be at work. A more competent layer at depth can lead to crater flattening as seen on the Moon, thereby decreasing *d/D* [e.g., 13]. Bennu's shape and topography implies a stiffness [4] that could be consistent with increased strength at depth.

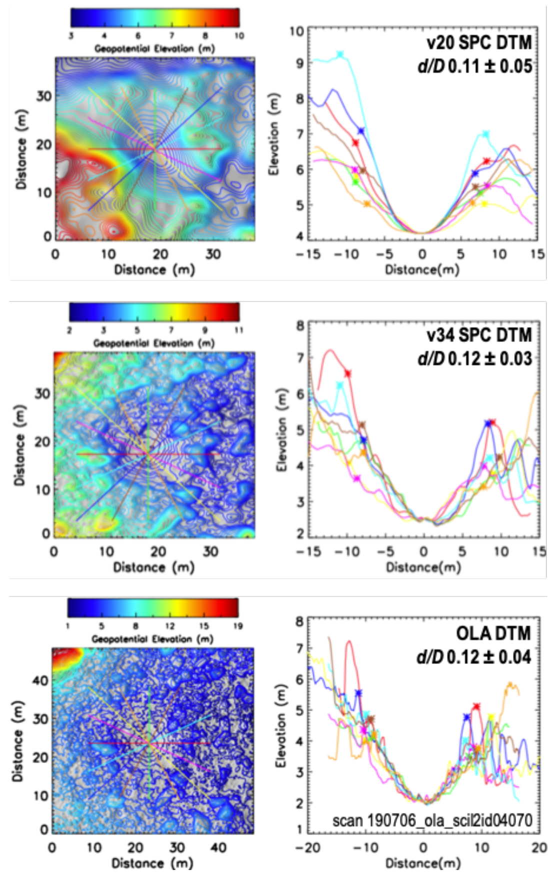

Figure 3. DTMs (left) and crater profiles (right) from a ~19 m crater at -0.63° N 315.07° E. All three DTMs lead to the same *d/D*, within error.

Acknowledgements: This material is based on work supported by NASA under contract NNM10AA11C issued through the New Frontiers Program. We are grateful to the entire OSIRIS-REx Team for making the encounter with Bennu possible.

References: [1] Bierhaus et al. (2019) *LPSC L,* abs. 2469. [2] Lauretta et al. (2019) *Nature*, 568, 55–60. [3] Scheeres et al. (2019) *Nat. Astron.* 3, 352–361. [4] Barnouin et al. (2019) *Nat. Geosci.,* 12, 247–252. [5] Walsh et al. (2019) *Nat. Geosci.,* 12, 242 – 246. [6] Hirata et al. (2009) *Icarus,* 200, 486–502. [7] Barnouin-Jha et al. (2001) *LPSC XXXII,* abs. 1786. [8] Sugita et al. (2019) *Science*, 364, eaaw0422. [9] Daly, R.T. et al. (2019) *LPSC L,* abs. 1647. [10] Barnouin et al. (2019) *Icarus,* 325, 67–83. [11] Schultz (1988) Cratering on Mercury: A Relook, *Mercury,* 19–91. [12] Nolan et al. (1996) *Icarus,* 124, 359–371. [13] Quaide and Oberbeck (1968) *JGR,* 73, 5247–5270.